

Chiral skyrmions of large radius

Stavros Komineas

Department of Mathematics and Applied Mathematics, University of Crete, 70013 Heraklion, Crete, Greece

Christof Melcher

Department of Mathematics & JARA Fundamentals of Future Information Technology, RWTH Aachen University, 52056 Aachen, Germany

Stephanos Venakides

Department of Mathematics, Duke University, Durham, NC, USA

Abstract

We study the structure of an axially symmetric magnetic skyrmion in a ferromagnet with the Dzyaloshinskii-Moriya interaction. We examine the regime of large skyrmions and we identify rigorously the critical value of the dimensionless parameter at which the skyrmion radius diverges to infinity, while the skyrmion energy converges to zero. This critical value coincides with the expected transition point from the uniform phase, which accommodates the skyrmion as an excited state, to the helical phase, which has negative energy. We give the profile field at the skyrmion core, its outer field, and the intermediate field at the skyrmion domain wall. Moreover, we derive an explicit formula for the leading asymptotic behavior of the energy as well as the leading term and first asymptotic correction for the value of the critical parameter. The key leading to the results is a parity theorem that utilizes exact formulae for the asymptotic behavior of the solutions of the static Landau-Lifshitz equation centered at the skyrmion domain wall. The skyrmion energy is shown to be an odd function of the radius and the dimensionless parameter to be an even function.

Keywords: Magnetic skyrmion, Micromagnetics, Dzyaloshinskii-Moriya interaction

2000 MSC: 49S05: Variational principles of physics, 35Q51: Solitons, 82D40: Magnetic materials,

34B15: Nonlinear boundary value problems

1. Introduction

Magnetic skyrmions are two-dimensional topological solitons $\mathbf{m} : \mathbb{R}^2 \cup \{\infty\} \rightarrow \mathbb{S}^2$ with $\deg \mathbf{m} = \pm 1$. After their theoretical prediction [1, 2] they have been observed in ferromagnets with the Dzyaloshinskii-Moriya (DM) interaction and techniques have been developed for individual skyrmions to be created and annihilated in a controlled manner [3]. DM interaction arises from the loss of chiral symmetry induced by the underlying crystal structure or due to thin-film or multilayer geometries. Chiral interaction terms and chiral skyrmions also arise in variational models for other condensed matter systems including spin-orbit coupled Bose-Einstein condensates (BEC) [4, 5] or nematic liquid crystals [6, 7].

Our model is based on a micromagnetic energy functional that includes exchange, DM and easy-axis anisotropy terms. The system can be described by a single dimensionless DM parameter ϵ , defined in Eq. (6), given as the ratio of the DM parameter divided by (half) the domain wall energy. It is known (though not rigorously proven yet) that, there are only two phases minimizing the energy per unit area: the

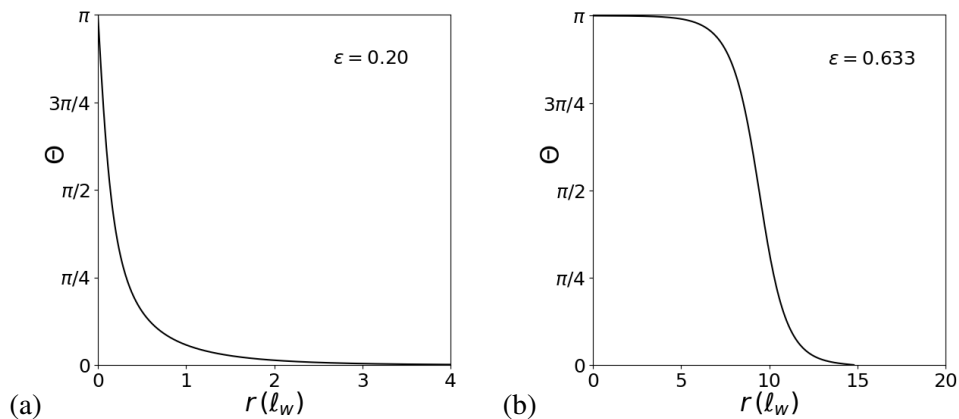


Figure 1: In contrast to the small skyrmion (a) being a localized perturbation of the Belavin-Polyakov soliton, the key feature of the large skyrmion (b) is a domain wall structure that separates the core from the far field. The slope of the profile approaches π exponentially in the limit of large radius.

uniform phase and the helical phase for small and for large DM parameter ϵ respectively [2]. The spiral state has negative energy and it is represented by one-dimensional (1D) modulations in the form of a distorted flat helix perpendicular to the helix propagation vector. This is a periodic solution of the 1D static Landau-Lifshitz equation. The transition from the spiral to the uniform state occurs at $\epsilon = 2/\pi$, and it is achieved as the period of the spiral goes to infinity for $\epsilon \rightarrow 2/\pi$.

The isolated chiral skyrmion is an excited state in the parameter regime of non-negative energy where the uniform state is the absolute energy minimizer. Most approaches are based on the assumption of axial symmetry so that \mathbf{m} is represented by its polar angle $\Theta = \Theta(r)$ depending on the radial coordinate $r > 0$. The existence of skyrmionic solutions as local minimizers of the micromagnetic energy has been rigorously proven for the case of an external field [8, 9]. The argument has been extended to the case of uniaxial anisotropy including stray-field interaction [10, 11], and to director models of chiral liquid crystals [12].

Skyrmionic solutions of the static Landau-Lifshitz equation in the presence of a DM term can be found by numerical methods [2, 13]. Numerical results provide the phase diagram for the existence of skyrmions and various features of the skyrmion profile. The skyrmion profile determines to a large extent, and sometimes crucially, the skyrmion properties [14]. Its details are thus essential for the manipulation of individual skyrmions. Skyrmions exhibit different morphologies depending on the size of ϵ , see Figure 1. For skyrmions of large radius, an ad-hoc ansatz based on explicit (1D) domain wall profiles [15] has been suggested and is widely used to examine structural and dynamic properties, see, e.g., [16, 17, 18]. In Ref. [19] a 1D profile with the domain wall width as an additional parameter is used. The profile enters in formulae for dynamical phenomena, for example, skyrmion translation and oscillation modes [20, 19] or antiferromagnetic skyrmion excitations [21], and it is crucial for quantitative calculations. In recent years, sufficient resolution has been obtained for the observation of the features of the skyrmion profile in great detail [16, 22, 13, 23, 24, 25, 26]. The availability of a detailed analytical description of the skyrmion profile is thus important and it will open the way for a wider exploitation of individual skyrmions.

For the case of skyrmions of small radius, analytic formulae for the profile of axisymmetric skyrmions have been derived [27]. In this asymptotic regime where the dimensionless DM parameter ϵ is small, magnetic skyrmions are well approximated on small scales by the classical Belavin-Polyakov soliton. The results in Ref. [27] provide a quantitative description of this approximation in terms of asymptotic formulae

for the skyrmion radius $R \sim \frac{\epsilon}{|\ln \epsilon|}$ and energy $E - 4\pi \sim \frac{\epsilon^2}{\ln \epsilon}$ for $\epsilon \ll 1$.

In this paper, we derive formulae for the skyrmion profile in the case of large skyrmion radius by employing asymptotic methods that give analytic approximations of the skyrmion solutions for the time-independent Landau-Lifshitz equation. Our analysis predicts a breakdown of skyrmions solutions, via a diverging radius, when approaching the threshold value $\epsilon = 2/\pi$ from below, and thereby supports its role as critical constant. We define the skyrmion radius R via $\Theta(R) = \pi/2$ and we write the angle Θ as an asymptotic series

$$\Theta = \Theta_0 + \frac{\Theta_1}{R} + \frac{\Theta_2}{R^2} + \frac{\Theta_3}{R^3} + \dots \quad (1)$$

It is customary to define a variable $T = R - r$ which shifts the origin from the center to the radius of the skyrmion, and to consider $\Theta = \Theta(T)$.

A key observation is the following parity property of the expansion (1). We show that the functions $\Theta_n(T)$ are odd functions of T if n is even; they are even functions, if n is odd. The angle Θ_0 coincides with the functional form of the 1D domain wall (Bloch wall), and the Θ_n , $n = 1, 2, \dots$ are asymptotic corrections. We also show that the DM parameter ϵ is expressed as the even asymptotic series

$$\epsilon = \epsilon_0 + \frac{\epsilon_2}{R^2} + \frac{\epsilon_4}{R^4} + \dots \quad (2)$$

We obtain $\epsilon_0 = 2/\pi$ (within the two-dimensional model) and this coincides with the value at which the transition from the ferromagnetic regime to the helical regime takes place. The numerical values of the coefficients ϵ_n , $n = 2, 4, \dots$ are calculated. Finally we show that the skyrmion energy E is expressed as the odd asymptotic series

$$E = \frac{E_1}{R} + \frac{E_3}{R^3} + \dots \quad (3)$$

The results of the present analysis for large radius, taken in combination with the results of Ref. [27] for small radius give a reasonably complete description of the skyrmion profile and energy depending on ϵ .

The paper is arranged as follows. In Section 2 we explain the mathematical model and present the equation for the skyrmion profile, while in subsection 2.1 we give the formulae for the skyrmion profile in the core and the outer region. In Section 3 we give a systematic method to obtain an asymptotic series for the skyrmion profile. In Section 4 we apply the theory of the previous section and obtain numerical values for the asymptotic formulae. In Section 5 we derive a Pohozaev identity and apply this to find explicit formulae for the ϵ vs R relation. In Section 6 we give an asymptotic expansion for the skyrmion energy. Appendix A contains the details of the calculations for the skyrmion profile in the core and in the outer region. Appendix B contains the proof of a theorem which establishes a fundamental parity property for the skyrmion profile. Appendix C contains the details of the calculations for the ϵ_2 and for the energy expansion.

2. The skyrmion equation

We consider a two-dimensional ferromagnet on the xy -plane with exchange, Dzyaloshinskii-Moriya interaction, and anisotropy of the easy-axis type perpendicular to the plane. The micromagnetic structure is described via the magnetization vector $\mathbf{m} = \mathbf{m}(x, y)$ with a fixed magnitude normalized to unity, $\mathbf{m}^2 = 1$. The normalized form of the micromagnetic energy reads [27]

$$E_\epsilon(\mathbf{m}) = \int \left[\frac{1}{2} \partial_\mu \mathbf{m} \cdot \partial_\mu \mathbf{m} + \frac{1}{2} (1 - m_3^2) + \epsilon e_{\text{DM}} \right] dx. \quad (4)$$

A summation over repeated indices $\mu = 1, 2$ is assumed. The last term in the parenthesis in Eq. (4) models the DM interaction. Prototypical cases are the bulk DM interaction form $e_{\text{DM}} = \hat{\mathbf{e}}_\mu \cdot (\partial_\mu \mathbf{m} \times \mathbf{m})$ and the

interfacial DM interaction form $e_{\text{DM}} = \epsilon_{\mu\nu} \hat{e}_\mu \cdot (\partial_\nu \mathbf{m} \times \mathbf{m})$, where $\epsilon_{\mu\nu}$ is the totally antisymmetric two-dimensional tensor. Here $\hat{e}_1, \hat{e}_2, \hat{e}_3$ are the unit vectors for the magnetization in the respective directions. Static magnetization configurations satisfy the static Landau-Lifshitz equation

$$\mathbf{m} \times (\partial_\mu \partial_\mu \mathbf{m} + m_3 \hat{e}_3 - 2\epsilon \mathbf{h}_{\text{DM}}) = 0. \quad (5)$$

where the last term is the DM field with $\mathbf{h}_{\text{DM}} = \hat{e}_\mu \times \partial_\mu \mathbf{m}$ in case of bulk interaction or $\mathbf{h}_{\text{DM}} = \epsilon_{\mu\nu} \hat{e}_\mu \times \partial_\nu \mathbf{m}$ in case of interfacial DM. In Eq. (4) and (5), lengths are measured in units of the domain wall width $\ell_w = \sqrt{A/K}$, where A is the exchange and K the anisotropy constant. The equation contains a single parameter

$$\epsilon = \frac{\ell_S}{\ell_w} = \frac{D}{2\sqrt{AK}} \quad (6)$$

defined via an additional length scale of this model $\ell_S = D/(2K)$, where D is the DM parameter (in Ref. [2], a parameter which differs from ϵ only by a constant factor has been introduced). We will refer to ϵ as the *dimensionless DM parameter*, but one should keep in mind that it can also be controlled by changing the anisotropy or the exchange parameter. The lowest energy (ground) state is the spiral for $\epsilon > 2/\pi$ and the ferromagnetic state for $\epsilon < 2/\pi$ [2].

Let us consider the angles (Θ, Φ) for the spherical parametrization of the magnetization vector, and the polar coordinates (r, ϕ) for the film plane. We assume an axially symmetric skyrmion with $\Phi = \phi + \phi_0$ and $\Theta = \Theta(r)$. For a bulk DM term the energy is minimized for $\phi_0 = \pi/2$ (Bloch skyrmion) and for interfacial DM interaction we choose $\phi_0 = 0$ (Néel skyrmion). A value $0 < \phi_0 < \pi/2$ should be chosen if the DM term is a combination of the bulk and interfacial terms.

The skyrmion profile arises as a local minimizer of the energy

$$E_\epsilon(\mathbf{m}) = 2\pi \int_0^\infty \left[\frac{1}{2} \left(\frac{d\Theta}{dr} \right)^2 + \frac{1}{2} \left(1 + \frac{1}{r^2} \right) \sin^2 \Theta + \epsilon \left(\frac{d\Theta}{dr} + \frac{1}{2r} \sin 2\Theta \right) \right] r dr \quad (7)$$

of

$$\mathbf{m}(r, \phi) = (\sin \Theta \cos(\phi + \phi_0), \sin \Theta \sin(\phi + \phi_0), \cos \Theta)$$

whereby $\Theta = \Theta(r)$ satisfies the equation

$$\Theta'' + \frac{\Theta'}{r} - \frac{\sin(2\Theta)}{2r^2} - \frac{\sin(2\Theta)}{2} + 2\epsilon \frac{\sin^2 \Theta}{r} = 0 \quad (8)$$

with boundary conditions $\Theta(0) = \pi$ and $\lim_{r \rightarrow \infty} \Theta(r) = 0$. The same equation applies to all types of skyrmions, e.g., Bloch and Néel skyrmions for the respective DM terms.

2.1. The skyrmion core and the outer region

We study skyrmions with large radius R , defined by the equation

$$\Theta(R) = \frac{\pi}{2}.$$

The skyrmion profile exhibits three spatial regions. The skyrmion core is the region where the value of Θ is close to π (magnetization pointing close to the south pole). The outer region (or far field) is where Θ is exponentially close to zero (magnetization pointing close to the north pole). The skyrmion domain wall is the thin region that connects the core and the outer region. Eq. (8) reduces to the modified Bessel equation both at the skyrmion core and in the far field and it is studied in Appendix A. Using asymptotic analysis,

we obtain the following results. Close to the skyrmion center, the deviation of the skyrmion profile from π is linear with an exponentially small factor (see Eqs. (A.4), (A.7)),

$$\Theta \approx \pi - e^{-R} \sqrt{2\pi R} r, \quad r \ll 1. \quad (9)$$

As r increases, the deviation attains exponential growth; this is held in check by the small factor throughout the skyrmion core, up to the approach to the domain wall (see Eqs. (A.5), (A.7)),

$$\Theta \approx \pi - 2 \sqrt{\frac{R}{r}} e^{r-R}, \quad 1 \ll r \ll R. \quad (10)$$

The leading approximation of the skyrmion domain wall profile is independent of the radius when the radius is large, (see Sec. 3). Past the domain wall, in the far field, the behavior is similar to the one of skyrmions of small radius [27]. We have (see Eqs. (A.9), (A.11))

$$\Theta \approx 2 \sqrt{\frac{R}{r}} e^{-(r-R)}, \quad r \gg R. \quad (11)$$

The core and the far field profiles are matched with the respective sides of the domain wall profile to leading order.

3. High order analysis of the skyrmion domain wall

We focus attention in the region of the skyrmion domain wall and develop an analysis valid to all orders in R^{-1} for skyrmions of large radius. The leading behavior of the solution as $R \rightarrow \infty$ is obtained by neglecting the terms of Eq. (8) with r in the denominator. The emerging equation

$$\Theta'' - \frac{1}{2} \sin(2\Theta) = 0 \quad (12)$$

characterizes the leading behavior of the domain wall of the skyrmion and has solution

$$\Theta_0 = 2 \arctan(e^{-T}), \quad (13)$$

where

$$T = r - R, \quad T \in (-R, \infty). \quad (14)$$

The constants of integration follow from the requirements $\Theta_0 = \frac{\pi}{2}$ when $T = 0$ and $\Theta_0 \rightarrow 0$ as $T \rightarrow \infty$. We calculate easily the following quantities that will be used below,

$$\Theta'_0 = -\operatorname{sech} T, \quad \cos(2\Theta_0) = 1 - 2 \operatorname{sech}^2 T, \quad \sin(2\Theta_0) = 2 \operatorname{sech} T \tanh T, \quad \sin^2 \Theta_0 = \operatorname{sech}^2 T. \quad (15)$$

Proceeding to a higher order analysis, we use the radius R as the parameter of the problem. We construct an asymptotic series for the profile Θ in negative powers of R to all orders. The profile $\Theta(T)$ is expanded to an asymptotic series for large R ,

$$\Theta = \Theta_0 + \tilde{\Theta}, \quad \tilde{\Theta} = \frac{\Theta_1}{R} + \frac{\Theta_2}{R^2} + \frac{\Theta_3}{R^3} + \dots \quad (16)$$

$\Theta_0(T)$ is given by Eq. (13) and $\Theta_1, \Theta_2, \Theta_3, \dots$ are also functions of T . Necessarily ϵ must be expressed in terms of the parameter R . We choose the same form of asymptotic expansion as for Θ ,

$$\epsilon = \epsilon_0 + \frac{\epsilon_1}{R} + \frac{\epsilon_2}{R^2} + \frac{\epsilon_3}{R^3} + \dots \quad (17)$$

We introduce the expansion

$$\frac{1}{r} = \frac{p}{T}, \quad p = \frac{T}{R} \left(1 - \frac{T}{R} + \frac{T^2}{R^2} + \dots \right). \quad (18)$$

The motivation for this notation is that p is a power series of the ratio T/R . We finally introduce the expansions of trigonometric functions isolating the leading order,

$$\cos(2\tilde{\Theta}) = 1 + C(2\tilde{\Theta}), \quad \sin(2\tilde{\Theta}) = 2\tilde{\Theta} + S(2\tilde{\Theta}) \quad (19)$$

where C, S contain the higher order terms of the Taylor expansions about zero of the cosine and sine functions, respectively. Inserting the series (16) for Θ into Eq. (8), applying the identities of trigonometric addition and using Eqs. (17), (18), (19) obtains

$$\tilde{\Theta}'' - \cos(2\Theta_0)\tilde{\Theta} = \tilde{g} \quad (20)$$

where the prime denotes differentiation with respect to T , and

$$\tilde{g} = \frac{g_1}{R} + \frac{g_2}{R^2} + \frac{g_3}{R^3} + \dots \quad (21)$$

The explicit form of \tilde{g} is given in Eq. (B.1). The hierarchy of linear nonhomogeneous equations for the functions Θ_n is obtained directly from Eq. (20),

$$\Theta_n'' - (\cos 2\Theta_0) \Theta_n = g_n, \quad n = 1, 2, 3, \dots \quad (22)$$

The forcing term g_n of the equation for Θ_n may depend only on the functions Θ_l with $l \leq n-1$. All equations have the same homogeneous part. All equations are given the initial condition $\Theta_n(T=0) = 0$.

The homogeneous equation corresponding to the hierarchy (22) is

$$\Theta_H'' - (1 - 2 \operatorname{sech}^2 T) \Theta_H = 0. \quad (23)$$

This equation describes the motion of a quantum mechanical particle in a potential well (see, e.g., Ref. [28], page 73). The potential equaling negative $\operatorname{sech}^2 T$ is one of the Bargmann reflectionless potentials, a class of potentials of the one-dimensional Schrödinger operator having bound states with negative energy and zero reflection coefficient for all positive energies [29]. Eq. (23) has the explicit basis solutions

$$H_1 = \operatorname{sech} T, \quad H_2 = \sinh T + T \operatorname{sech} T. \quad (24)$$

Their Wronskian is given by

$$\det \begin{pmatrix} H_1 & H_2 \\ H_1' & H_2' \end{pmatrix} = 2. \quad (25)$$

Using the formula of the variation of constants, we obtain

$$\Theta_n = -\frac{1}{2}H_1(T) \int_0^T g_n(\tau)H_2(\tau) d\tau + \frac{1}{2}H_2(T) \int_{-\infty}^T g_n(\tau)H_1(\tau) d\tau, \quad n = 1, 2, 3, \dots \quad (26)$$

This solution satisfies the boundary condition $\Theta_n(0) = 0$ and the solvability condition (boundary condition at infinity)

$$\int_{-\infty}^{\infty} g_n(\tau)H_1(\tau) d\tau = 0, \quad n = 1, 2, 3, \dots \quad (27)$$

The condition is the consequence of the fact that Eq. (22) for Θ_n has the form $\mathbb{L}\Theta_n = g_n$, where \mathbb{L} is a selfadjoint differential operator. Since $H_1(T)$ is in its nullspace, the inner product $(g_n, H_1) = (\mathbb{L}\Theta_n, H_1) = (\Theta_n, \mathbb{L}H_1) = 0$.

The calculation of the Θ_n is recursive; in order to demonstrate the calculational pattern, we examine the explicit form of the functions g_1, g_2, g_3

$$\begin{aligned} g_1 &= -(\Theta'_0 + 2\epsilon_0 \sin^2 \Theta_0) \\ g_2 &= T(\Theta'_0 + 2\epsilon_0 \sin^2 \Theta_0) - 2\epsilon_1 \sin^2 \Theta_0 + \sin 2\Theta_0 \left(\frac{1}{2} - 2\epsilon_0 \Theta_1 - \Theta_1^2 \right) - \Theta'_1 \\ g_3 &= -T^2(\Theta'_0 + 2\epsilon_0 \sin^2 \Theta_0) + 2(T\epsilon_1 - \epsilon_2) \sin^2 \Theta_0 + T\Theta'_1 - \Theta'_2 \\ &\quad + \sin 2\Theta_0 [-T + (T\epsilon_0 - \epsilon_1)2\Theta_1 - 2\epsilon_0\Theta_2 - 2\Theta_1\Theta_2] + \cos 2\Theta_0 \left(\Theta_1 - 2\epsilon_0\Theta_1^2 - \frac{2}{3}\Theta_1^3 \right). \end{aligned} \quad (28)$$

We make the following observations

1. Θ_0 is an odd function of T , thus, g_1 is even. Inserting g_1 into the solvability condition (27), produces the value of ϵ_0 .
2. The fact that g_1 in Eq. (26) is even implies that also Θ_1 is even.
3. All the terms of g_2 are odd with the exception of the term multiplied by ϵ_1 , which is even. Inserting g_2 into the solvability condition (27), produces $\epsilon_1 = 0$. Thus, g_2 is odd.
4. The fact that g_2 in Eq. (26) is odd implies that also Θ_2 is odd.
5. All terms of g_3 are even. Inserting g_3 into the solvability condition (27) produces the value of ϵ_2 .

The cycle continues periodically according to the flow chart

$$\underbrace{\Theta_0}_{\text{odd}} \rightarrow \underbrace{g_1}_{\text{even}} \rightarrow \underbrace{\begin{Bmatrix} \epsilon_0 \\ \Theta_1 \end{Bmatrix}}_{\text{even}} \rightarrow \underbrace{g_2}_{\text{odd}} \rightarrow \underbrace{\begin{Bmatrix} \epsilon_1 = 0 \\ \Theta_2 \end{Bmatrix}}_{\text{odd}} \rightarrow \underbrace{g_3}_{\text{even}} \rightarrow \underbrace{\begin{Bmatrix} \epsilon_2 \\ \Theta_3 \end{Bmatrix}}_{\text{even}} \rightarrow \underbrace{g_4}_{\text{odd}} \rightarrow \underbrace{\begin{Bmatrix} \epsilon_3 = 0 \\ \Theta_4 \end{Bmatrix}}_{\text{odd}} \rightarrow \dots$$

with odd indexed g_n and Θ_n being even and even indexed g_n and Θ_n being odd.

The coefficient ϵ_n makes its first appearance in the expression of g_{n+1} multiplying the term $-2 \operatorname{sech}^2 T$ for every n . Using this, the solvability condition (27) produces the values

$$\epsilon_n = \frac{1}{\pi} \int_{-\infty}^{\infty} (\operatorname{sech} \tau) g_{n+1}(\tau)|_{\epsilon_n=0} d\tau, \quad n = 0, 1, 2, 3, \dots \quad (29)$$

For every odd n the integrand is odd giving $\epsilon_n = 0$, i.e., all odd indexed ϵ_n vanish. As a result, relation (17) of the dimensionless DM parameter with the skyrmion radius is simplified to

$$\epsilon = \epsilon_0 + \frac{\epsilon_2}{R^2} + \frac{\epsilon_4}{R^4} + \frac{\epsilon_6}{R^6} + \dots \quad (30)$$

The parity results stated here are proved in the following theorem.

Theorem 1. *Let $\epsilon_{2i-1} = 0$ for $i = 1, 2, 3, \dots$. Then, the following parity conditions hold.*

1. *For all $n \geq 1$, the functions $g_n = g_n(T)$ are even if n is odd and they are odd if n is even.*
2. *The same is true for the functions $\Theta_n = \Theta_n(T)$, for $n \geq 0$.*

The theorem is instrumental for the following calculations. Its proof, involving some subtlety, is relegated to Appendix B in order to allow the flow of the calculation to be continued uninterrupted.

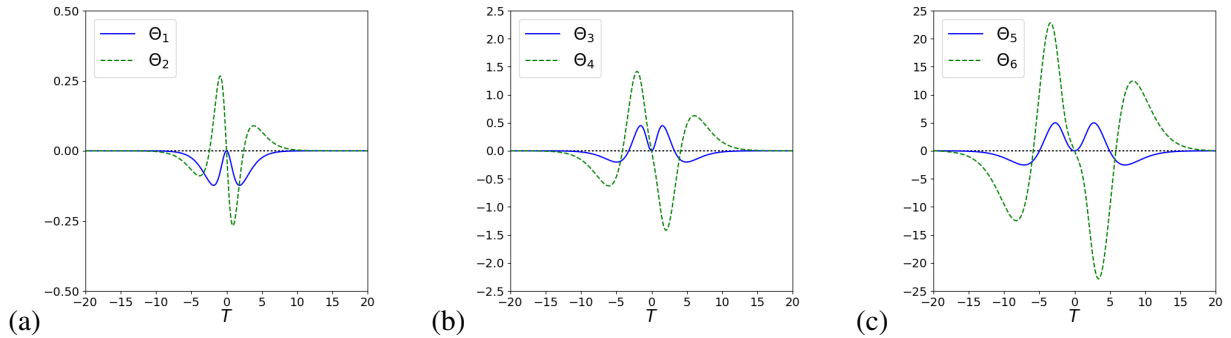


Figure 2: The functions (a) Θ_1, Θ_2 , (b) Θ_3, Θ_4 , and (c) Θ_5, Θ_6 calculated by numerical evaluation of the integrals in Eq. (26). As seen by the change of scale of the vertical axis in the three entries, the values of the functions Θ_n increase fast with increasing index n . Note the even parity of the odd indexed functions and the odd parity of the even indexed ones with respect to the variable $T = r - R$.

4. Numerics

We proceed to find $\Theta_1, \Theta_2, \Theta_3, \Theta_4, \Theta_5, \Theta_6$ by applying Eq. (26). The expressions for g_n for higher n are long and they have been derived using the mathematics software system SageMath [30]. The derivatives Θ'_n needed in the expressions of g_n are found by finite differences in the numerical calculation. Fig. 2 shows functions Θ_1 through Θ_6 . As expected from Theorem 1, odd indexed Θ_n 's are even functions of T and even indexed ones are odd. Functions Θ_n with higher index n take higher values and they take significant values over larger intervals of T . These features have consequences for the quality of the approximation, especially for small R , as we shall see in the following.

We have calculated by a shooting method the skyrmion profiles, which are solutions of Eq. (8), for various values of the parameter ϵ . (We have actually solved an equation for the stereographic projection of the magnetization vector which is equivalent to Eq. (8), as described in Ref. [27].) They are shown in Fig. 3 by small circles for two values of the parameter ϵ . In Fig. 3a, we have $\epsilon = 0.60$ that gives a skyrmion of radius $R = 3.29 \ell_w$. The profile at the skyrmion core is approximated very well by the solution given in Eq. (A.4) with the coefficient given in Eq. (A.7), and is shown as an orange dashed line in the figure. The blue solid line shows the one-dimensional domain wall profile Θ_0 , shown in Eq. (13), centred at the skyrmion radius position $r = R$. The red line shows the series solution (16) for Θ up to the term $O(1/R^6)$. The approximation of the skyrmion profile is excellent for all r except near the skyrmion center $r = 0$. In Fig. 3b, we have $\epsilon = 0.55$ and a smaller skyrmion radius $R = 2.02 \ell_w$. The solution (A.4) still gives an excellent approximation at the skyrmion core. The green line shows the series solution (16) for Θ up to the term $O(1/R^2)$ and obtains a good approximation of the profile, especially around the skyrmion radius and for $r > R$. The terms of the series (16) of order higher than $O(1/R^2)$ cannot be used to improve the approximation, and they rather give larger deviations from the true profile if added to the series. This phenomenon could have already been anticipated given the form of the Θ_n 's shown in Fig. 2 and the observation that an increasing index n gives Θ_n 's with rapidly increasing values. When a term Θ_n/R^n is larger than the previous term in the series the series should be truncated omitting this term.

We now calculate the numerical values of ϵ_n from Eq. (29). We obtain

$$\epsilon \approx \frac{2}{\pi} - \frac{0.3057}{R^2} - \frac{0.8792}{R^4} - \frac{5.901}{R^6}, \quad R \gg 1, \quad (31)$$

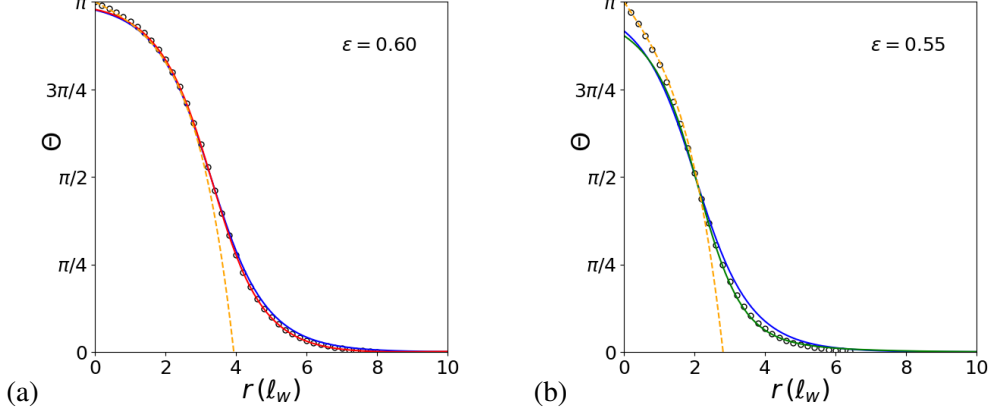


Figure 3: The profile of a skyrmion $\Theta(r)$ is shown by small circles for two values of the parameter ϵ , obtained numerically by solving the original Eq. (8) using a shooting method. The blue line shows Θ_0 , which is the one-dimensional domain wall profile. The orange line shows the solution (A.4) for the skyrmion profile at the core, obtained by linearizing the original equation about $\Theta = \pi$. (a) For $\epsilon = 0.60$ the skyrmion has a radius $R = 3.29 \ell_w$, as obtained by the shooting method. The red line shows the series (16) summed up to the term Θ_6 . (b) For $\epsilon = 0.55$ the skyrmion has a radius $R = 2.02 \ell_w$. For this smaller value of R the optimal point of truncation of the series occurs at the term Θ_2 . The green line shows the series (16) summed up to and including the term Θ_2 .

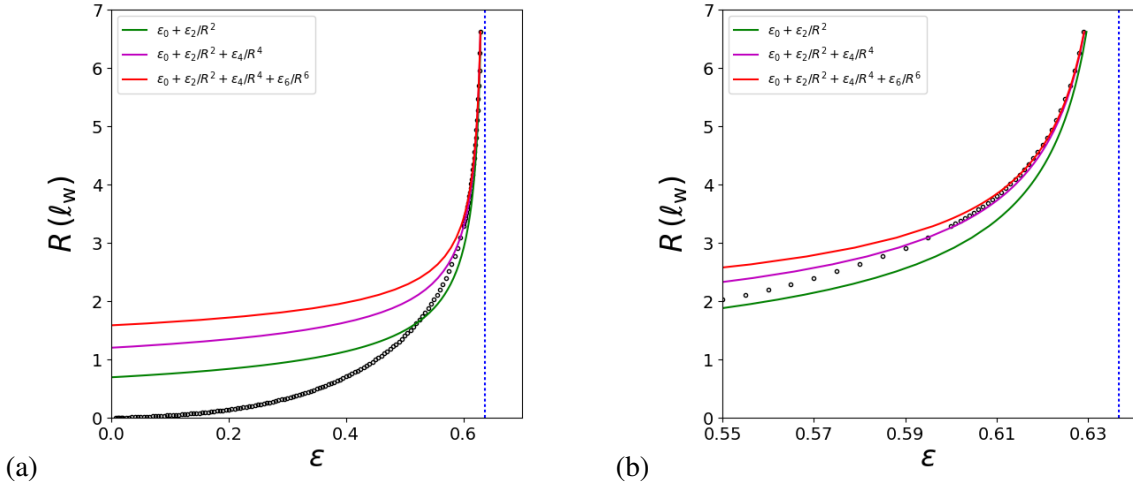


Figure 4: (a) The skyrmion radius R found numerically by solving the original equation (8) for various values of ϵ is shown by open circles. Relation (31) is shown by the colored lines to order $O(1/R^2)$, $O(1/R^4)$, $O(1/R^6)$ as indicated in the legend. The dotted blue line is an asymptote and marks the critical value $\epsilon = 2/\pi$. The successive approximations enhance the accuracy as R increases. (b) A blow-up of the graph for the region of large values of R .

where

$$\epsilon_0 = \frac{1}{\pi} \int_{-\infty}^{\infty} \operatorname{sech}^2 \tau \, d\tau = \frac{2}{\pi} \quad (32)$$

is obtained analytically while

$$\epsilon_2 \approx -0.3057, \quad \epsilon_4 \approx -0.8792, \quad \epsilon_6 \approx -5.901 \quad (33)$$

are found by numerical integration. Inverting Eq. (30) we obtain the skyrmion radius versus the parameter ϵ ,

$$R = \frac{|\epsilon_2|^{1/2}}{\tilde{\epsilon}^{1/2}} + O(\tilde{\epsilon}^{1/2}), \quad \tilde{\epsilon} = \frac{2}{\pi} - \epsilon. \quad (34)$$

Fig. 4 shows by open circles the skyrmion radius extracted from the calculation of the skyrmion profiles by the shooting method. These data are compared with formula (31) for the successive approximations up to and including order $O(1/R^2)$, $O(1/R^4)$, and $O(1/R^6)$. The approximation is excellent for large R and it is improving as we add higher order terms, as seen in the blow-up in Fig. 4b. For smaller R , higher order approximations give larger deviations from the correct result, especially when the term $O(1/R^6)$ is included. This is a consequence of the increasing error in the asymptotic series for small values of R as was discussed in relation to Fig. 3.

5. A Pohozaev type identity and an explicit form of ϵ_2

We multiply Eq. (8) by $2r\Theta'$ and we integrate over the r axis. After straightforward algebraic and trigonometric manipulations, we obtain

$$\int_0^{\infty} \left[(r\Theta'^2)' + \Theta'^2 - \left(r + \frac{1}{r} \right) (\sin^2 \Theta)' + 4\epsilon (\sin^2 \Theta)\Theta' \right] dr = 0. \quad (35)$$

The first and last terms under the integral are exact derivatives; they integrate to zero and to $-2\pi\epsilon$ respectively. Performing an integration by parts, we obtain the Pohozaev type identity that is satisfied by all skyrmions and is crucial for our calculation,

$$\int_0^{\infty} \left[\Theta'^2 + \left(1 - \frac{1}{r^2} \right) \sin^2 \Theta \right] dr = 2\pi\epsilon. \quad (36)$$

The following theorem, based on relation (36), provides an explicit formula for ϵ_2 and an alternative derivation of ϵ_0 .

Theorem 2. *The DM parameter ϵ satisfies the relation*

$$\epsilon = \frac{2}{\pi} - \frac{1}{\pi R^2} \left(1 + \frac{1}{2} \int_{-\infty}^{\infty} \Theta_1 g_1 dT \right) + O(R^{-4}). \quad (37)$$

Proof. We take the limit $R \rightarrow \infty$ in the integral law (36). The integral of $\sin^2 \Theta/r^2$ converges to zero; the integrand decays exponentially in the core and outer region of the skyrmion. In the limit, we are left with

$$\int_{-\infty}^{\infty} (\Theta_0'^2 + \sin^2 \Theta_0) dT = 2\pi\epsilon_0. \quad (38)$$

The integral in Eq. (38) is calculated using Eqs. (15) and equals 4. The critical value $\epsilon_0 = 2/\pi$ follows directly.

For the determination of ϵ_2 we expand the Pohozaev identity (36) in powers up to $O(R^{-2})$. We insert $\Theta = \Theta_0 + \tilde{\Theta}$, and make T the integration variable. The manipulation, which involves integrations by parts resulting in significant cancellations, is relegated to Appendix C.1. We obtain

$$\epsilon_2 = -\frac{1}{\pi} \left(1 + \frac{1}{2} \int_{-\infty}^{\infty} \Theta_1 g_1 dT \right). \quad (39)$$

The value of the latter integral is found in Appendix C.3. Inserting the value given in Eq. (C.16) into Eq. (39) we find

$$\epsilon_2 = -\frac{0.9605}{\pi} \approx -0.3057 \quad (40)$$

It agrees with the result in Eq. (33) found by a different method in Sec. 4. \square

In Ref. [31], the value $\epsilon_2 = -1/\pi$ was found by an energy minimization argument that takes only Θ_0 into account.

6. Energy of skyrmion

Let us denote by $E_{\text{ex}}, E_{\text{an}}, E_{\text{DM}}$ the exchange, anisotropy and DM energy terms in the total energy (7). Using a standard scaling argument [32] one proves that any localized configuration that is a minimum of the energy in an infinitely extended two-dimensional system, such as a skyrmion, satisfies

$$2E_{\text{an}} + E_{\text{DM}} = 0. \quad (41)$$

In a one dimensional system the same argument gives for minima of the energy, such as a domain wall,

$$E_{\text{ex}} - E_{\text{an}} = 0. \quad (42)$$

In the limit $\epsilon \rightarrow 2/\pi$, the latter relation is correct to leading order also for a skyrmion, as the leading approximation for the skyrmion profile, in this limit, is Θ_0 . Thus, in the limit, a skyrmion satisfies both (41) and (42), and these are combined to give

$$E_{\text{ex}} = E_{\text{an}} = -\frac{E_{\text{DM}}}{2} \quad \text{when } \epsilon \rightarrow \frac{2}{\pi}. \quad (43)$$

The total skyrmion energy is

$$E = E_{\text{ex}} + E_{\text{an}} + E_{\text{DM}} = 0 \quad \text{when } \epsilon \rightarrow \frac{2}{\pi}. \quad (44)$$

We give a full asymptotic series for the energy in the following theorem.

Theorem 3. *All three forms of skyrmion energy in Eq. (7), exchange, anisotropy and DM, have asymptotic expansions in which only odd powers of R are present,*

$$E_{\text{ex}} = 2\pi R + \frac{E_{\text{ex},1}}{R} + \frac{E_{\text{ex},3}}{R^3} + \dots, \quad E_{\text{an}} = 2\pi R + \frac{E_{\text{an},1}}{R} + \frac{E_{\text{an},3}}{R^3} + \dots, \quad E_{\text{DM}} = -4\pi R + \frac{E_{\text{DM},1}}{R} + \frac{E_{\text{DM},3}}{R^3} + \dots, \quad (45)$$

The three leading terms sum up to zero; the total energy is

$$E \sim \frac{E_1}{R} + \frac{E_3}{R^3} + \frac{E_5}{R^5} + \dots, \quad E_1 = 4\pi^2 |\epsilon_2|, \quad R \rightarrow \infty. \quad (46)$$

The skyrmion energy tends to zero, as ϵ increases, approaching its critical value, with a rate of convergence

$$E \sim (4\pi^2 |\epsilon_2|^{1/2}) \tilde{\epsilon}^{1/2} + O(\tilde{\epsilon}^{3/2}), \quad \tilde{\epsilon} = \frac{2}{\pi} - \epsilon. \quad (47)$$

Proof. We classify the functions of the form $f(T)R^n$, where the function f can be odd or even and the power n can be any integer, according to the following table.

Class	n	f
A	odd	even
B	even	odd
C	odd	odd
D	even	even

It suffices to prove that every term of the expression under the energy integral (7) belongs to class $A + B + C$. The integration will eliminate the terms in B and C ; only odd powers of R will participate in the expression of each of the three components of the energy and, hence, in the total energy.

In order to simplify the notation, we use the symbol of the class to also denote the class elements as well as sums of the class elements. Thus,

$$\Theta_0 + \frac{\Theta_2}{R^2} + \frac{\Theta_4}{R^4} + \dots \equiv B, \quad \frac{\Theta_1}{R} + \frac{\Theta_3}{R^3} + \frac{\Theta_5}{R^5} + \dots \equiv A, \quad T \equiv B, \quad R \equiv A. \quad (48)$$

We notice that

$$A^2 \equiv B^2 \equiv C^2 \equiv D^2 \equiv D, \quad AB \equiv C, \quad AC \equiv B, \quad BC \equiv A, \quad AD \equiv A, \quad BD \equiv B, \quad A' \equiv C, \quad B' \equiv D. \quad (49)$$

We also have

$$\sin A \equiv A, \quad \sin B \equiv B, \quad \cos A \equiv \cos B \equiv D. \quad (50)$$

By applying trigonometric identities, we obtain

$$\sin(A + B) \equiv AD + BD \equiv A + B, \quad \cos(A + B) \equiv DD + AB \equiv D + C. \quad (51)$$

We perform the calculation term by term, expressing $\sin^2 \Theta$ as $\frac{1}{2}(1 - \cos 2\Theta)$.

1. Term $r \left(\frac{d\Theta}{dr} \right)^2 \equiv (R + T)(A + B)^2 \equiv (A + B)(C^2 + CD + D^2) \equiv (A + B)(D + C) \equiv A + B$.
2. Term $r \frac{d\Theta}{dr} \equiv (A + B)(C + D) \equiv A + B$.
3. Term $\sin 2\Theta \equiv \sin(A + B) \equiv \sin(A + B) \equiv A + B$.
4. Term $r + \frac{1}{r} \equiv A + B$ (see Eq. (18)).
5. Term $\left(r + \frac{1}{r} \right) \cos 2\Theta \equiv (A + B)(D + C) \equiv A + B$.

This shows that only odd powers of R are present.

The highest order term in the energy is $O(R)$ with the contributions of the three energy terms (exchange, anisotropy and DM) given by the corresponding three terms in the integral

$$2\pi R \int_{-\infty}^{\infty} \left\{ \frac{1}{2} \left(\frac{d\Theta_0}{dT} \right)^2 + \frac{1}{2} \sin^2 \Theta_0 + \frac{2}{\pi} \left(\frac{d\Theta_0}{dT} \right) \right\} dT. \quad (52)$$

Inserting the relevant quantities from Eqs. (15), we obtain the $O(R)$ terms in Eq. (45) for the individual energies. The $O(R)$ term in the total energy vanishes. The term $O(R^{-1})$ is calculated in Appendix C.2, giving the result of Eq. (46). Inserting Eq. (34) into Eq. (46), we obtain Eq. (47). \square

Acknowledgement

We are grateful to Stefan Blügel and to Alex Bogdanov for fruitful discussions. CM gratefully acknowledges financial support by the DFG under the grant no. ME 2273/3-1, and SK a Mercator fellowship as part of the previous grant. SV gratefully acknowledges financial support by the NSF through contract DMS-1211638. SK acknowledges funding from the Hellenic Foundation for Research and Innovation (HFRI) and the General Secretariat for Research and Technology (GSRT), under grant agreement No 871.

Appendix A. The skyrmion core and the outer region

We derive the leading asymptotic behaviors of Θ in the skyrmion core ($-R < T < 0$, $|T| \gg 1$) and in the outer region ($T > 0$, $|T| \gg 1$) and match them with the expressions of Θ obtained for the domain wall. Matching occurs on the overlap layers $1 \ll |T| \ll R$, with $T < 0$ on the left and $T > 0$ on the right. The leading asymptotic on the overlap layers obtained from the domain wall's Eq. (13) is

$$\Theta \sim \begin{cases} \pi - 2e^{-|T|}, & T < 0 \\ 2e^{-|T|}, & T > 0. \end{cases} \quad (\text{A.1})$$

The skyrmion core (Region A)

In the spatial region from $r = 0$ and up to the domain wall, we have

$$\theta(r) = \pi - \Theta(r) \ll 1, \quad \sin \theta \sim \theta. \quad (\text{A.2})$$

The DM term in Eq. (8) is clearly subdominant ($\theta^2 \ll \theta$) and is neglected. In terms of θ , Eq. (8) becomes the modified Bessel equation

$$r^2 \theta'' + r\theta' - (r^2 + 1)\theta = 0, \quad \theta(0) = 0. \quad (\text{A.3})$$

We will use its series solution $I_1(r)$ which equals zero at $r = 0$ (this is the modified Bessel function of the first kind, see [33], par. 9.6.10),

$$\theta = C_1 I_1(r), \quad I_1(r) = \frac{r}{2} \sum_{n=0}^{\infty} \frac{\left(\frac{1}{4}r^2\right)^n}{n!(n+1)!}, \quad (\text{A.4})$$

where C_1 is a constant. The large r behavior of the function $I_1(r)$ is (see [33], par. 9.7.1)

$$I_1(r) \sim \frac{e^r}{\sqrt{2\pi r}} \left(1 - \frac{3}{8r} + \dots\right). \quad (\text{A.5})$$

The constant C_1 is now evaluated by identifying the leading asymptotic deviation from π of the angle Θ on the overlapping layer of the region A and the domain wall,

$$\Theta(r) \sim \begin{cases} \pi - C_1 \frac{e^r}{\sqrt{2\pi r}} \sim \pi - C_1 \frac{e^R}{\sqrt{2\pi R}} e^{-|T|}, & T < 0, |T| \gg 1 \text{ (Region A, Modified Bessel)}, \\ \pi - 2e^{-|T|}, & |T| \ll R \text{ (Domain wall)}. \end{cases} \quad (\text{A.6})$$

We obtain

$$C_1 = e^{-R} \sqrt{8\pi R}. \quad (\text{A.7})$$

The slope of the skyrmion profile at its center $r = 0$ is

$$\frac{d\Theta}{dr}(r=0) = -e^{-R} \sqrt{2\pi R}. \quad (\text{A.8})$$

The skyrmion outer region (region B)

As in region A, the DM term may be neglected. The angle $\Theta(r)$ then satisfies the modified Bessel equation (A.3). The appropriate solution is $K_1(r)$ (modified Bessel function of the second kind) which decays as $r \rightarrow \infty$. Since $r \gg 1$ in this region, we only need the asymptotic behavior of $K_1(r)$ (see [33], par. 9.7.2)

$$\Theta = C_2 K_1(r), \quad K_1(r) \sim \sqrt{\frac{\pi}{2r}} e^{-r} \left(1 - \frac{3}{8r} + \dots \right), \quad (\text{A.9})$$

where C_2 is a constant.

The constant C_2 is evaluated by identifying the leading behavior of the angle Θ on the overlapping layer of the region B and the domain wall,

$$\Theta(r) \sim \begin{cases} C_2 \sqrt{\frac{\pi}{2r}} e^{-r} \sim C_2 \sqrt{\frac{\pi}{2R}} e^{-R} e^{-|T|}, & T > 0, T \gg 1 \text{ (Region B, Modified Bessel)}, \\ 2e^{-|T|}, & T \ll R \text{ (Domain wall)}. \end{cases} \quad (\text{A.10})$$

Matching the leading order terms of the formulae for Θ in the overlapping region gives

$$C_2 = \sqrt{\frac{8R}{\pi}} e^R. \quad (\text{A.11})$$

Appendix B. Parity theorem

Proceeding to the calculation at higher orders of $1/R$ we determine the formula for \tilde{g} utilizing Eqs. (18), (19). We obtain

$$\begin{aligned} \tilde{g} = & -p \frac{\Theta'_0}{T} - p\epsilon \frac{1 - \cos(2\Theta_0)}{T} + p^2 \frac{\sin(2\Theta_0)}{2T^2} - p \frac{\tilde{\Theta}'}{T} + \left(-p\epsilon \frac{\sin(2\Theta_0)}{T} + p^2 \frac{\cos(2\Theta_0)}{2T^2} \right) 2\tilde{\Theta} \\ & + \left(\frac{1}{2} \sin(2\Theta_0) + p\epsilon \frac{\cos(2\Theta_0)}{T} + p^2 \frac{\sin(2\Theta_0)}{2T^2} \right) C(2\tilde{\Theta}) + \left(\frac{1}{2} \cos(2\Theta_0) - p\epsilon \frac{\sin(2\Theta_0)}{T} + p^2 \frac{\cos(2\Theta_0)}{2T^2} \right) S(2\tilde{\Theta}). \end{aligned} \quad (\text{B.1})$$

The following theorem is instrumental for all calculations based on Eq. (22), and in particular for those presented in Sec. 3. The hypotheses of the theorem turn out to be necessary conditions for the existence of bounded solutions Θ_n .

Theorem. Let $\epsilon_{2i-1} = 0$ for $i = 1, 2, 3, \dots$. Then, the following parity conditions hold.

1. For all $n \geq 1$, the functions $g_n = g_n(T)$ are even if n is odd and they are odd if n is even.
2. The same is true for the functions $\Theta_n = \Theta_n(T)$.

Proof. When g_n is odd, it follows directly from Eq. (26) that Θ_n is also odd. When g_n is even, the first two terms on the right side of Eq. (26) are even; the last term is odd and exponentially increasing therefore $c_{n,2}$ must be set to zero. As a result Θ_n is even. Therefore, it suffices to prove the theorem for the g_n . We already know that the theorem is true for $n = 1$.

Clearly, only terms Θ_j with $j < n$ appear in the expression for g_n , so we can truncate $\tilde{\Theta}$ accordingly. We make the inductive assumption that the functions $g_1, g_2, g_3, \dots, g_{n-1}$ and hence the functions

$\Theta_1, \Theta_2, \Theta_3, \dots, \Theta_{n-1}$ alternate in parity, with g_1 and Θ_1 being even functions of T . We prove that the theorem is then true for $g_1, g_2, g_3, \dots, g_n$ and hence for $\Theta_1, \Theta_2, \Theta_3, \dots, \Theta_n$. We recall that Θ_0 is an odd function of T . We define for convenience

$$\delta = \frac{1}{R}$$

and we observe that p is a power series of (δT) .

We show that g_n satisfies the parity condition term by term. The condition is true for the first term, namely, $p\Theta'_0/T$. Indeed, p must be represented by $(\delta T)^n$ for the term to be of order δ^n . The term becomes $T^{n-1}\Theta'_0$, which satisfies the parity condition since Θ'_0 is even. In a similar way, the parity law is satisfied for the remaining two terms in which no Θ_j appears. The verification for the terms in which only one Θ_j appears is equally straightforward. For example, if in the term before the first parenthesis, p is represented by $(\delta T)^m$, the term is $T^{m-1}\Theta'_{n-m}\delta^n$. The parity requirement is clearly satisfied for $m = 1$, since taking the derivative changes the parity. Increasing the value of m by k introduces k factors T and also shifts the index of Θ backwards by k positions. According to our inductive assumption, the parity of the term is preserved.

More work is required to show that the parity condition holds for the terms that have the factor $C(\tilde{\Theta})$ or $S(\tilde{\Theta})$. According to the inductive assumption, the truncated

$$\tilde{\Theta} = \delta\Theta_1 + \delta^2\Theta_2 + \delta^3\Theta_3 + \dots + \delta^{n-1}\Theta_{n-1} \quad (\text{B.2})$$

has even functions of T multiplying the odd powers of δ and odd functions of T multiplying the even powers of δ . The general term of the expansions of $C(\tilde{\Theta})$ and $S(\tilde{\Theta})$ is represented by

$$\tilde{\Theta}^{\mathbf{k}} = (2\delta)^{\mathbf{k}\cdot\mathbf{q}}\Theta_1^{k_1}\Theta_2^{k_2}\dots\Theta_{n-1}^{k_{n-1}}, \quad (\text{B.3})$$

where $\mathbf{k} = (k_1, k_2, k_3, \dots, k_{n-1})$ with $k_i \in \{0, 1, 2, 3, \dots\}$, and where $\mathbf{q} = (1, 2, 3, \dots, n-1)$. The term $\tilde{\Theta}^{\mathbf{k}}$ is either even or odd, since the factors Θ_j are even or odd.

Claim.

- (a) All the terms in the expansion of $C(\tilde{\Theta})$ are even at even powers of δ and odd at odd powers of δ .
- (b) All the terms in the expansion of $S(\tilde{\Theta})$ are odd at even powers of δ and even at odd powers of δ .

In order to prove the claim, we utilize the notion of the parity of a number or a function. The parity equals zero in the case of evenness and it equals unity in the case of oddness of the number or function. We calculate the following three parities.

- (i) The parity of the exponent n in the order δ^n of a term $\tilde{\Theta}^{\mathbf{k}}$.
- (ii) The parity of the product $\Theta_1^{k_1}\Theta_2^{k_2}\dots\Theta_{n-1}^{k_{n-1}}$ in $\tilde{\Theta}^{\mathbf{k}}$.
- (iii) The parity of the number of the factors Θ_j in $\tilde{\Theta}^{\mathbf{k}}$, counting multiplicities.

We obtain the following.

- (i) The exponent of δ equals $n = \mathbf{k} \cdot \mathbf{q}$. For the calculation of the parity of n , we set $k_j q_j = 0$ if q_j is even (eliminates all the odd factors Θ_j) or if k_j is even (eliminates all factors Θ_j with even multiplicity). We are thus, keeping only the even factors with odd multiplicity. The parity is thus

$$N_{\text{even}} \equiv \# \text{ of factors } \Theta_j \text{ that are even functions with odd multiplicity mod}(2). \quad (\text{B.4})$$

- (ii) The second parity, which we denote by N_{odd} , equals

$$N_{\text{odd}} \equiv \# \text{ of odd factors with odd multiplicity mod}(2). \quad (\text{B.5})$$

- (iii) The parity of the number of the factors Θ_j in $\tilde{\Theta}^{\mathbf{k}}$, counting multiplicities is given by the sum $k_1 + k_2 + \dots + k_{n-1}$. It is an even number for the terms of $C(\tilde{\Theta})$ and an odd number for the terms of $S(\tilde{\Theta})$. The third parity, which we denote by N_{total} , equals

$$N_{\text{total}} \equiv \# \text{ of all factors of odd multiplicity mod}(2). \quad (\text{B.6})$$

Clearly, $N_{\text{even}} + N_{\text{odd}} \equiv N_{\text{total}} \pmod{2}$. Hence, $N_{\text{total}} \equiv 0$ in the case of $C(\tilde{\Theta})$ and $N_{\text{total}} \equiv 1$ for $S(\tilde{\Theta})$. Parities 1 and 2 agree with each other in the terms of $C(\tilde{\Theta})$ and differ from each other in the terms of $S(\tilde{\Theta})$. This proves the claim.

Now that the parity of the terms of C and S are understood, the correctness of the theorem for the terms involving these is verified similarly to the previous terms.

Appendix C. Detailed calculations for ϵ_2 and for the energy expansion

Appendix C.1. A formula for ϵ_2

For the determination of ϵ_2 we expand the identity (36) in powers up to $O(R^{-2})$. Inserting $\Theta = \Theta_0 + \tilde{\Theta}$, and passing to T as the integration variable, we obtain

$$\int_{-\infty}^{\infty} \left[(\Theta'_0 + \tilde{\Theta}')^2 + \left(1 - \frac{1}{R^2}\right) \sin^2(\Theta_0 + \tilde{\Theta}) \right] dT = 2\pi \left(\epsilon_0 + \frac{\epsilon_2}{R^2} \right) + O(R^{-4}). \quad (\text{C.1})$$

We calculate

$$(\Theta'_0 + \tilde{\Theta}')^2 = \Theta_0'^2 + \frac{1}{R} 2\Theta'_0 \Theta'_1 + \frac{1}{R^2} (2\Theta'_0 \Theta'_2 + \Theta_1'^2) + O(R^{-3}) \quad (\text{C.2})$$

and

$$\begin{aligned} \sin^2(\Theta_0 + \tilde{\Theta}) &= (\sin \tilde{\Theta} \cos \Theta_0 + \cos \tilde{\Theta} \sin \Theta_0)^2 \\ &= \sin^2 \Theta_0 + \frac{1}{R} \Theta_1 \sin 2\Theta_0 + \frac{1}{R^2} (\Theta_1^2 \cos 2\Theta_0 + \Theta_2 \sin 2\Theta_0) + O(R^{-3}). \end{aligned} \quad (\text{C.3})$$

We insert these results into Eq. (C.1). The terms $O(1)$ cancel due to Eq. (38). The $O(R^{-1})$ terms are odd and vanish upon integration. The terms $O(R^{-3})$ vanish for the same reason. The $O(R^{-2})$ terms give

$$\int_{-\infty}^{\infty} (2\Theta'_0 \Theta'_2 + \Theta_2 \sin 2\Theta_0 + \Theta_1'^2 + \Theta_1^2 \cos 2\Theta_0 - \sin^2 \Theta_0) dT = 2\pi \epsilon_2. \quad (\text{C.4})$$

We perform an integration by parts in the first and third terms,

$$\int_{-\infty}^{\infty} [\Theta_2 (\sin 2\Theta_0 - 2\Theta_0'') - \Theta_1 (\Theta_1'' - \Theta_1 \cos 2\Theta_0) - \sin^2 \Theta_0] dT = 2\pi \epsilon_2. \quad (\text{C.5})$$

The first parenthesis vanishes due to Eq. (12) and the second one is equal to g_1 due to Eq. (22). We obtain

$$- \int_{-\infty}^{\infty} (\Theta_1 g_1 + \sin^2 \Theta_0) dT = 2\pi \epsilon_2. \quad (\text{C.6})$$

We integrate the second term in the left side by using Eq. (15) and obtain

$$\epsilon_2 = -\frac{1}{\pi} \left(1 + \frac{1}{2} \int_{-\infty}^{\infty} \Theta_1 g_1 dT \right) \quad (\text{C.7})$$

proving a result in Theorem 2. The value of the latter integral is found in Appendix C.3.

Appendix C.2. A formula for the leading order energy

We address the exchange, anisotropy and DM terms under the energy integral (7) separately. The arrows below indicate that only terms $O(R^{-1})$ are taken. They also allow replacement of a term by an equal quantity, omitting terms that integrate to zero, and operations corresponding to integration by parts, for example Θ_1^2 being replaced by $-\Theta_1'\Theta_1$.

- Exchange:

$$\begin{aligned} \frac{1}{2}(R+T)\Theta'^2 + \frac{1}{2}\frac{\sin^2\Theta}{R+T} &: \mapsto \frac{1}{2}\Theta_1'^2 + \Theta_0'\Theta_2' + T\Theta_0'\Theta_1' + \frac{1}{2}\sin^2\Theta_0 \\ &\mapsto -\frac{1}{2}\Theta_1''\Theta_1 - \Theta_0''\Theta_2 - T\Theta_0''\Theta_1 - \Theta_0'\Theta_1 + \frac{1}{2}\sin^2\Theta_0. \end{aligned} \quad (\text{C.8})$$

- Anisotropy:

$$\frac{1}{2}(R+T)\sin^2\Theta : \mapsto \frac{1}{2}\Theta_1^2 \cos 2\Theta_0 + \frac{1}{2}\Theta_2 \sin 2\Theta_0 + \frac{1}{2}T\Theta_1 \sin 2\Theta_0. \quad (\text{C.9})$$

- DM:

$$\begin{aligned} (R+T)\left(\epsilon_0\Theta' + \frac{\epsilon_2}{R^2}\Theta'\right) + \frac{1}{2}\epsilon_0 \sin 2\Theta &: \mapsto \epsilon_0\Theta_2' + \epsilon_0T\Theta_1' + \epsilon_2\Theta_0' + \epsilon_0\Theta_1 \cos 2\Theta_0 \\ &\mapsto -\epsilon_0\Theta_1 + \epsilon_2\Theta_0' + \epsilon_0\Theta_1 \cos 2\Theta_0 \\ &\mapsto \epsilon_2\Theta_0' - 2\epsilon_0\Theta_1 \sin^2\Theta_0. \end{aligned} \quad (\text{C.10})$$

The second and third terms in the anisotropy cancel one by one the corresponding exchange terms in view of Eq. (12). The first term in the anisotropy combines with the first term in the exchange to give $-\frac{1}{2}\Theta_1g_1$ in view of (22). We are left with

$$\begin{aligned} &-\frac{1}{2}\Theta_1g_1 - (\Theta_0' + 2\epsilon_0 \sin^2\Theta_0)\Theta_1 + \epsilon_2\Theta_0' + \frac{1}{2}\sin^2\Theta_0 \\ &\mapsto \frac{1}{2}\Theta_1g_1 + \epsilon_2\Theta_0' + \frac{1}{2}\sin^2\Theta_0. \end{aligned}$$

We take the integral

$$\int_{-\infty}^{\infty} \left(\frac{1}{2}\Theta_1g_1 + \epsilon_2\Theta_0' + \frac{1}{2}\sin^2\Theta_0\right) dT = \frac{1}{2} \int_{-\infty}^{\infty} \Theta_1g_1 dT - \epsilon_2\pi + 1$$

and use (39) to obtain

$$E_1 = 4\pi \left(1 + \frac{1}{2} \int_{-\infty}^{\infty} \Theta_1g_1 dT\right) = 4\pi^2|\epsilon_2|. \quad (\text{C.11})$$

Appendix C.3. Evaluation of the integral in the expressions for ϵ_2 and E_1

We will evaluate the integral appearing in Eqs. (39), (C.7) for ϵ_2 and in Eq. (C.11) for E_1 . For $n = 1$, the solvability condition (27) is equivalent to

$$\int_0^{\infty} g_1(\tau)H_1(\tau) d\tau = 0, \quad (\text{C.12})$$

as a result of the evenness of the integrand. It follows that the lower limit $-\infty$ in Eq. (26) may be replaced with a zero lower limit; the integral in Eq. (39) is then written as

$$\int_{-\infty}^{\infty} \Theta_1g_1 dT = -\frac{1}{2} \int_{-\infty}^{\infty} dT g_1(T)H_1(T) \int_0^T d\tau g_1(\tau)H_2(\tau) + \frac{1}{2} \int_{-\infty}^{\infty} dT g_1(T)H_2(T) \int_0^T d\tau g_1(\tau)H_1(\tau). \quad (\text{C.13})$$

The two terms on the right in Eq. (C.13) are shown to be equal if we apply integration by parts and use the solvability condition (C.12). We have

$$\int_{-\infty}^{\infty} \Theta_1 g_1 dT = \int_{-\infty}^{\infty} dT g_1(T) H_2(T) \int_0^T d\tau g_1(\tau) H_1(\tau). \quad (\text{C.14})$$

The integral on the right can be calculated explicitly,

$$\int_0^T g_1(\tau) H_1(\tau) d\tau = \tanh T - \frac{2}{\pi} \tanh T \operatorname{sech} T - \frac{4}{\pi} \arctan(e^T) + 1. \quad (\text{C.15})$$

This is inserted into Eq. (C.14) and the integral is evaluated numerically to find

$$\int_{-\infty}^{\infty} \Theta_1 g_1 dT = -0.0790. \quad (\text{C.16})$$

References

- [1] A. N. Bogdanov and D. A. Yablonskii. Thermodynamically stable “vortices” in magnetically ordered crystals. The mixed state of magnets. *Sov. Phys. JETP*, 68:101–103, 1989.
- [2] A. N. Bogdanov and A. Hubert. Thermodynamically stable magnetic vortex states in magnetic crystals. *J. Magn. Magn. Mater.*, 138:255, 1994.
- [3] N. Romming, C. Hanneken, M. Menzel, J. E. Bickel, B. Wolter, K. von Bergmann, A. Kubetzka, and R. Wiesendanger. Writing and deleting single magnetic skyrmions. *Science*, 341(6146):636–639, 2013.
- [4] Amandine Aftalion and Peter Mason. Phase diagrams and thomas-fermi estimates for spin-orbit-coupled bose-einstein condensates under rotation. *Phys. Rev. A*, 88:023610, Aug 2013.
- [5] Amandine Aftalion and Rémy Rodiac. One dimensional phase transition problem modeling striped spin orbit coupled bose-einstein condensates. *Journal of Differential Equations*, 269:38–81, 2020.
- [6] Paul J. Ackerman, Rahul P. Trivedi, Bohdan Senyuk, Jao van de Lagemaat, and Ivan I. Smalyukh. Two-dimensional skyrmions and other solitonic structures in confinement-frustrated chiral nematics. *Phys. Rev. E*, 90:012505, Jul 2014.
- [7] David C. Wright and N. David Mermin. Crystalline liquids: the blue phases. *Rev. Mod. Phys.*, 61:385–432, Apr 1989.
- [8] C. Melcher. Chiral skyrmions in the plane. *Proc. R. Soc. A*, 470:20140394, October 2014.
- [9] X. Li and C. Melcher. Stability of axisymmetric chiral skyrmions. *J. Funct. Anal.*, 275(10):2817–2844, 2018.
- [10] Anne Bernand-Mantel, Cyrill B Muratov, and Thilo M Simon. A quantitative description of skyrmions in ultrathin ferromagnetic films and rigidity of degree ± 1 harmonic maps from \mathbb{R}^2 to \mathbb{S}^2 . *arXiv preprint arXiv:1912.09854*, 2019.
- [11] Anne Bernand-Mantel, Cyrill B. Muratov, and Thilo M. Simon. Unraveling the role of dipolar versus dzyaloshinskii-moriya interactions in stabilizing compact magnetic skyrmions. *Phys. Rev. B*, 101:045416, Jan 2020.
- [12] Carlo Greco. On the existence of skyrmions in planar liquid crystals. *Topological Methods in Nonlinear Analysis*, 2019.
- [13] A O Leonov, T L Monchesky, N Romming, A Kubetzka, A N Bogdanov, and R Wiesendanger. The properties of isolated chiral skyrmions in thin magnetic films. *New Journal of Physics*, 18:065003, 2016.
- [14] Karin Everschor-Sitte, J. Masell, R. M. Reeve, and M. Kläui. Perspective: Magnetic skyrmions—overview of recent progress in an active research field. *J. Appl. Phys.*, 124:240901, 2018.
- [15] H.-B. Braun. Fluctuations and instabilities of ferromagnetic domain-wall pairs in an external magnetic field. *Physical Review B*, 50(22):16485, 1994.
- [16] N. Romming, A. Kubetzka, C. Hanneken, K. von Bergmann, and R. Wiesendanger. Field-dependent size and shape of single magnetic skyrmions. *Phys. Rev. Lett.*, 114:177203, May 2015.
- [17] Y. Zhou, E. Iacocca, A. A. Awad, R. K. Dumas, F. C. Zhang, H.-B. Braun, and J. Åkerman. Dynamically stabilized magnetic skyrmions. *Nature communications*, 6:8193, 2015.
- [18] F. Büttner, I. Lemesch, and S. D. G. Beach. Theory of isolated magnetic skyrmions: From fundamentals to room temperature applications. *Sci. Rep.*, 8:4464, 2018.
- [19] Volodymyr P. Kravchuk, Denis D. Sheka, Ulrich K. Röbber, Jeroen van den Brink, and Yuri Gaididei. Spin eigenmodes of magnetic skyrmions and the problem of the effective skyrmion mass. *Phys. Rev. B*, 97:064403, Feb 2018.
- [20] C. Schütte and M. Garst. Magnon-skyrmion scattering in chiral magnets. *Phys. Rev. B*, 90:094423, Sep 2014.

- [21] Volodymyr P. Kravchuk, Olena Gomonyi, Denis D. Sheka, Davi R. Rodrigues, Karin Everschor-Sitte, Jairo Sinova, Jeroen van den Brink, and Yuri Gaididei. Spin eigenexcitations of an antiferromagnetic skyrmion. *Phys. Rev. B*, 99:184429, May 2019.
- [22] Olivier Boulle, Jan Vogel, Hongxin Yang, Stefania Pizzini, Dayane de Souza Chaves, Andrea Locatelli, Tevfik Onur Menteş, Alessandro Sala, Liliana D. Buda-Prejbeanu, Olivier Klein, Mohamed Belmeguenai, Yves Roussigné, Andrey Stashkevich, Salim Mourad Chérif, Lucia Aballe, Michael Foerster, Mairbek Chshiev, Stéphane Auffret, Ioan Mihai Miron, and Gilles Gaudin. Room-temperature chiral magnetic skyrmions in ultrathin magnetic nanostructures. *Nat. Nano.*, 11(5):449–454, may 2016.
- [23] D McGrouther, R J Lamb, M Krajnak, S McFadzean, S McVitie, R L Stamps, A O Leonov, A N Bogdanov, and Y Togawa. Internal structure of hexagonal skyrmion lattices in cubic helimagnets. *New Journal of Physics*, 18(9):095004, sep 2016.
- [24] A. Kovács, J. Caron, A. S. Savchenko, N. S. Kiselev, K. Shibata, Zi-An Li, N. Kanazawa, Y. Tokura, S. Blügel, and R. E. Dunin-Borkowski. Mapping the magnetization fine structure of a lattice of Bloch-type skyrmions in an FeGe thin film. *Applied Physics Letters*, 111(19):192410, 2017.
- [25] K. Shibata, A. Kovács, N. S. Kiselev, N. Kanazawa, R. E. Dunin-Borkowski, and Y. Tokura. Temperature and magnetic field dependence of the internal and lattice structures of skyrmions by off-axis electron holography. *Physical Review Letters*, 118(8):087202, 2017.
- [26] Sebastian Meyer, Marco Perini, Stephan von Malottki, André Kubetzka, Roland Wiesendanger, Kirsten von Bergmann, and Stefan Heinze. Isolated zero field sub-10 nm skyrmions in ultrathin Co films. *Nat. Comm.*, 10:3823, Aug 2019.
- [27] Stavros Komineas, Christof Melcher, and Stephanos Venakides. The profile of chiral skyrmions of small radius. *arXiv*, page 1904.01408, 2019.
- [28] L. D. Landau and E. M. Lifshitz. *Quantum Mechanics*. Pergamon Press, Oxford, second edition, 1965.
- [29] S. Novikov, S. V. Manakov, L. P. Pitaevskii, and V. E. Zhakharov. *Theory of solitons*. Plenum Publishing Corporation, New York, 1984.
- [30] The Sage Developers. *SageMath, the Sage Mathematics Software System (Version 8.7)*, 2019. <https://www.sagemath.org>.
- [31] S. Rohart and A. Thiaville. Skyrmion confinement in ultrathin film nanostructures in the presence of Dzyaloshinskii-Moriya interaction. *Phys. Rev. B*, 88:184422, Nov 2013.
- [32] G. H. Derrick. Comments on nonlinear wave equations as models for elementary particles. *J. Math. Phys.*, 5:1252, 1964.
- [33] Milton Abramowitz and Irene A. Stegun. *Handbook of Mathematical Functions with Formulas, Graphs, and Mathematical Tables*. Dover, New York, ninth dover printing, tenth gpo printing edition, 1964.